Development, formulation, and cellular mechanism of a lipophilic copper chelator for the treatment of Wilson's disease

Laura Gauthier, Peggy Charbonnier, Mireille Chevallet, Pascale Delangle, Isabelle Texier, Christelle Gateau, Aurélien Deniaud

Development, formulation, and cellular mechanism of a lipophilic copper chelator for the treatment of Wilson's disease

Laura Gauthier[a,b], Peggy Charbonnier[c], Mireille Chevallet[c], Pascale Delangle[a], Isabelle Texier[b,*], Christelle Gateau[a,*], Aurélien Deniaud[c,*]

[a] Univ. Grenoble Alpes, CEA, CNRS, IRIG-SyMMES, F-38000 Grenoble, France ;

[b] Univ. Grenoble Alpes, CEA, LETI-DTBS, F-38000 Grenoble, France ;

[c] Univ. Grenoble Alpes, CNRS, CEA, IRIG - Laboratoire de Chimie et Biologie des Métaux, F-38000 Grenoble, France ;

***** Corresponding author: aurelien.deniaud@cea.fr

***** Corresponding author: christelle.gateau@free.fr

***** Corresponding author: isabelle.texier-nogues@cea.fr

Abstract

Copper homeostasis is finely regulated in human to avoid any detrimental impact of free intracellular copper ions. Upon copper accumulation, biliary excretion is triggered in liver thanks to trafficking of the ATP7B copper transporter to bile canaliculi. However, in Wilson's disease this protein is mutated leading to copper accumulation. Current therapy uses Cu chelators acting extracellularly and requiring a life-long treatment with side effects. Herein, a new Cu(I) pro-chelator was encapsulated in long-term stable nanostructured lipid carriers. Cellular assays revealed that the pro-chelator protects hepatocytes against Cu-induced cell death. Besides, the cellular stresses induced by moderate copper concentrations, including protein unfolding, are counteracted by the pro-chelator. These data showed the pro-chelator efficiency to deliver intracellularly an active chelator that copes with copper stress and surpasses current and under development chelators. Although its biological activity is more mitigated, the pro-chelator nanolipid formulation led to promising results. This innovative approach is of outmost importance in the quest of better treatments for Wilson's disease.

Keywords: Wilson's disease, Hepatocytes, Copper chelator, Nanolipid formulation

1. Introduction

Copper is an essential trace element for Human with a relatively short half-life in the body of about one month. Following intestinal absorption, copper is delivered to the liver, which is the master regulator of organismal copper homeostasis. Indeed, on the one hand, liver provides circulating copper in different forms, but, on the other hand, it drives the excretion of excess copper through the bile. In the reducing intracellular environment, copper is mainly found in the +I redox state, but the shuttling between Cu(I) and Cu(II) is used in numerous enzymes performing redox reactions such as the mitochondrial cytochrome c oxidase. To avoid oxidative stress but also protein unfolding (Saporito-Magriñá et al., 2018), copper trafficking is tightly regulated from its cellular entry by a number of copper chaperones. These processes lead to less than one free copper atom per cell (Rae et al., 1999). In hepatocytes, the chaperone Atox1 is delivering copper to the ATP-dependent Cu-ATPase ATP7B, a membrane protein that is central for copper homeostasis. In basal conditions, ATP7B transports copper to the Golgi apparatus for maturation of ceruloplasmin, while upon copper excess ATP7B migrates to bile canaliculi to enable copper excretion (Polishchuk et al., 2014). In Wilson's disease, the gene coding for ATP7B is mutated leading to copper homeostasis disruption including this excretion mechanism, which triggers copper accumulation mainly in the liver and the brain (for review see (Członkowska et al., 2018; Lutsenko, 2014)).

This disease, described firstly by Wilson in 1912, is a human autosomal recessive genetic disorder (Wilson, 1912). The current therapeutic options to manage copper overload in

Wilson's disease treatment have been unchanged since the sixties. The main treatments, D-penicillamine (D-pen) and trientine, are copper chelating drugs that promote copper excretion mainly into urine. However, the use of these chelators for Wilson's disease requires a life-long treatment with frequent administration that exhibits serious side effects leading to limited treatment compliance. It is therefore crucial to develop new copper chelating drugs to maximize copper lowering effect, reduce side effects and improve patient's compliance. Besides, a drug with intracellular delivery may be of special interest. Since 2014, bis-choline-tetrathiomolybdate (TTM), a copper chelator with high affinity for Cu(I), has been produced and successfully tested in phase II clinical trials, and is currently in phase III but its safety is not proven yet (Weiss et al., 2017).

To improve Wilson's disease therapy, various initiatives are ongoing. Several of them are focused on the design and evaluation of new efficient copper chelating drugs, namely DPM-1001 (Krishnan et al., 2018), methanobactin (Lichtmannegger et al., 2016), and brain-targeted trientine thanks to liposomes (Tremmel et al., 2016). Besides, gene therapy strategies are also progressing (Murillo et al., 2019, 2016), as well as correctors of ATP7B that partially restore copper excretion activity (Allocca et al., 2018; Ji and Shen, 2010; van den Berghe et al., 2009).

Since more than ten years, we have designed a series of bioinspired chelators taking advantage of the high affinity of sulfur donors for Cu(I) (Delangle and Mintz, 2012; Jullien et al., 2013, 2014, 2015, Pujol et al., 2009, 2011b). These chelators are based on a nitrilotriacetic acid (NTA) scaffold extended by either three cysteines (Pujol et al., 2009,

2011b) or three D-penicillamine (Jullien et al., 2014). These chelators bind efficiently and selectively copper in the +I oxidation state in respect to other essential metal ions. This work has been extended to the design of liver targeted pro-chelators, which combine one of the previously described Cu(I) chelator with several GalNAc moieties. These prodrugs promote efficient ASGPR-mediated uptake into hepatocytes and deliver the efficient copper chelator (Gateau and Delangle, 2014; Monestier et al., 2016; Pujol et al., 2012, 2011a). Recently, preclinical studies on *atp7b*$^{-/-}$ mice showed that these products constitute a promising therapeutic option to fight copper overload in Wilson's disease (Monestier et al., 2020).

A strategy to maximize the efficiency of copper chelators by promoting their specific hepatic targeting after *in vivo* administration could rely on the use of lipid nanovectors. This strategy would have the advantages of protecting the active molecule upon delivery before its release inside hepatocytes, of favouring prolonged distribution within the body, and of reducing side effects. Nanostructured Lipid Carriers (NLC) developed in the early 2000s by Müller (H. Muller et al., 2011; Mehnert, 2001) and Gasco (Cavalli et al., 1996) are lipid nanoparticles consisting of a core of mixed solid and liquid lipids, and a surfactant shell. They are particularly attractive as lipid nanocarriers due to their long-term colloidal stability, their efficient encapsulation of lipophilic compounds, and their up-scalable fabrication process (Beloqui et al., 2016; Carbone et al., 2014; Doktorovová et al., 2016; Müller et al., 2002; Sawant and Dodiya, 2008; Teixeira et al., 2017). NLC have since then aroused high interest as drug delivery systems, and in particular for liver targeting (Kong et al., 2013; Liu et al., 2014), all the more that they can be formulated for the oral delivery route (Liu et al., 2014;

Nasirizadeh and Malaekeh-Nikouei, 2020; Tan et al., 2020; Wang et al., 2015). Recently, a new generation of NLC based on FDA approved ingredients has been developed by our team and demonstrated great promise for imaging purposes (Sayag et al., 2016; Vigne et al., 2020), and the delivery of active pharmaceutical ingredients (Bayon et al., 2018; Michy et al., 2019; Tezgel et al., 2018). In particular, their biodistribution pattern evidenced important liver uptake and metabolization (Gauthier et al., 2021; Merian et al., 2013), underlining their potential as efficient nanocarriers for liver treatments.

These preliminary results therefore conducted us to explore the potentiality of NLC to efficiently drive into hepatocytes copper-chelating prodrugs derived from the previously described bioinspired Cu(I) chelators (Gateau and Delangle, 2014; Jullien et al., 2015, 2014, 2013, Pujol et al., 2012, 2011a, 2009) (Figure 1). For this purpose, a novel version of our most efficient chelator, the tripodal pseudopeptide NTA($CysNH_2$)$_3$ (Pujol et al., 2011b) was designed in the form of the lipophilic prodrug NTA(Cys(COC_8H_{17})NH_2)$_3$ **3** (Figure 1) thanks to the use of a thioesther bond. NLC were efficiently loaded with the pro-chelator **3** providing a stable **3**-NLC formulation efficiently endocytosed by hepatocytes. The biological activity of NTA(Cys(COC_8H_{17})NH_2)$_3$ **3** and **3**-NLC was then tested in HepG2/C3a cells and compared to chelators presently used and in development for treatments, *i.e.* D-pen, trientine and TTM. NTA(Cys(COC_8H_{17})NH_2)$_3$ **3** proved to be a very efficient compound *in cellulo* to cope with copper stress while being safer compared to other chelators and moderate effect was observed with its encapsulated version, **3**-NLC.

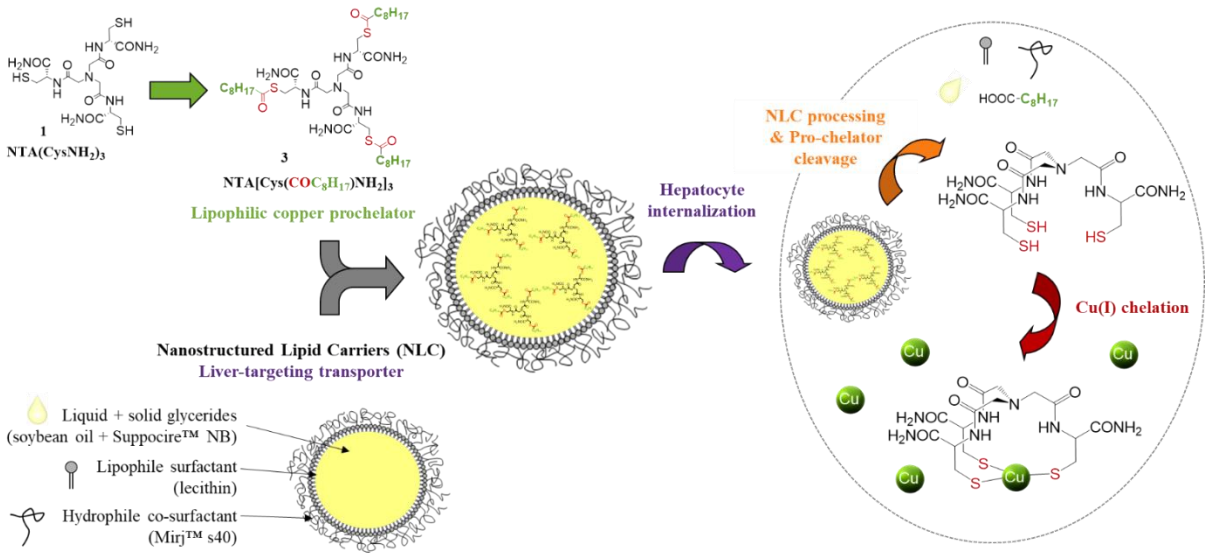

Figure 1. Novel strategy for the targeted delivery of copper-chelating prodrug.

2. Material and methods

2.1. Chemicals

Solvents and reagents were purchased from Sigma Aldrich, Acros, Alfa Aesar, Carlo Erba, Fluka, and VWR, and were used without further purification unless specified. $NTA(CysNH_2)_3$ was obtained according to already published procedure (Pujol et al., 2011b). Suppocire™ NB were purchased from Gattefossé (Saint-Priest, France). Myrj™ S40 (poly(ethylene glycol) stearate surfactant with 40 ethylene glycol motifs), and Super-refined Soybean oil™ were supplied by CRODA (Chocques, France). Lipoid s75™ was purchased from Lipoid GmbH (Ludwigshafen, Germany). SpectraPor dialysis membrane 12-14,000 Da was purchased from Roth Sochiel EURL (Lauterbourg, France).

2.2. Synthesis of NTA[Cys(COC_8H_{17})NH_2]$_3$ ***3***

To a solution of nonanoic acid (0.318 g, 2.01 mmol, 5 eq.) in CH_2Cl_2 (40mL), triethylamine (0.56 mL, 4.02 mmol, 10 eq.) was added. After stirring for 10 min, PyBOP (1.05 g, 2 mmol, 5 eq.) was added to the reaction mixture and the solution was stirred at room temperature under argon for 2 hours. Then NTA($CysNH_2$)$_3$ (0.200 g, 0.402 mmol, 1 eq.) was added to the mixture and stirring was maintained during 5 days. The resulting mixture was concentrated under reduced pressure and precipitation was obtained upon addition of cold diethyl ether. Resulting solid was rinsed with water (3 x 20 mL) and ethanol (3 x 5 mL). NTA[Cys(COC_8H_{17})NH_2]$_3$ **3** was obtained as a white electrostatic powder (97 mg, 26%).

^{1}H NMR and ^{13}C NMR spectra were recorded on a Bruker Avance 400 spectrometer. Chemical shifts (δ) were reported in ppm with the solvent as the internal reference, except for ^{13}C NMR spectra in D_2O, which were referenced to external DSS. Mass spectra were acquired with a Finigan LXQ-linear ion trap (THERMO Scientific, San Jose, USA) equipped with an electrospray source.

^{1}H NMR (DMSO-d^6, 400 MHz, 298 K): δ ppm = 8.36 (d, J = 8.6 Hz, 3H, 3xNH); 7.45 (s, 3H, 3xNH_2); 7.22 (s, 3H, 3xNH_2); 4.35 (t, J = 4.6 Hz, 3H, 3xCH), 3.38-3.22 (m, 6H, 3xCH_2); 3.01 (dd, J = 8.6, 13.3 Hz, 6H, 3xCH_2); 2.56-2.47 (m, 6H, 3xCH_2); 1.53 (t, J=6.9 Hz, 6H, 3xCH_2); 1.23 (s broad, 30H, 15xCH_2 aliphatic chain); 0.85 (t, J = 6.9 Hz, 9H, 3xCH_3).

^{13}C NMR (DMSO-d^6, 100 MHz, 298 K): δ ppm = 198.20 (3xSCO), 171.52, 170.45 (6xCO), 57.39 (3xCH), 51.53, 43.33, 43.11, 31.23, 30.39, 28.65, 28.52 ,28.27, 25.03 and 22.07 (27xCH_2), 13.95 (3xCH_3)

ES-MS: calculated mass: 917.5; found m/z: 918.4 $[M+H]^+$; 940.5 $[M+Na]^+$

Analytical RP-HPLC: purity = 88.5%. For quantitation, a calibration curve plotting $NTA(Cys(COC_8H_{17})NH_2)_3$ **3** peak area *versus* compound **3** concentration was established using 6 concentrations from 0.03 to 1.1 mM, each being performed in triplicates. $NTA(Cys(COC_8H_{17})NH_2)_3$ was quantitatively detected by UV absorbance at 235 nm in this concentration range. The calibration curve and fitted equation are reported in Figure S1.

2.3. *NLC formulation*

The lipid phase was prepared by mixing solid (Suppocire™ NB, 245 mg) and liquid (Super-refined Soybean oil™, 85 mg) glycerides, lipophilic surfactant Lipoid s75™ (65 mg), and when required compound **3** (13.5 mg), as well as DiD (800 nmol in 200 µL ethanol) to obtain fluorescently labeled NLC for fluorescence microscopy and flow cytometry experiments. The aqueous phase was composed of the hydrophilic surfactant, Myrj™ S40 (345 mg), and 1X PBS aqueous buffer (100 mM phosphate, NaCl 10 mM, pH 7.4, qsp 2 mL). After homogenization at 45°C, both lipid and aqueous phases were crudely mixed and sonication cycles were performed at 45°C during 5 minutes with a VCX750 Ultrasonic sonication probe (power output 190 W, 3-mm probe diameter, Sonics). Non-encapsulated components were separated from NLC by dialysis (1X PBS, MWCO: 12 kDa, overnight). Prior to characterization, NLC dispersions were filtered through a 0.22 µm cellulose Millipore membrane. Particle concentration was assessed by weighting freeze-dried samples of NLC obtained from a known volume (typically, 300 µL).

2.4. Dynamic Light Scattering Measurements

NLC hydrodynamic diameter and zeta potential were measured at 22°C with a Malvern Zeta Sizer Nano instrument (NanoZS, Malvern, UK) in 0.1X PBS buffer. Physical stability was investigated by DLS measurements with samples stored at 4°C (lipid dispersed phase weight fraction during storage: 10%). At least three different NLC batches were used per condition. Mean average diameters and polydispersity indices reported were obtained from scattered light intensity results. Data were expressed in terms of mean and standard deviation of all the samples for each condition, each sample result being the mean of three independent measurements performed at 25°C.

*2.5. Sample preparation for the quantification of NTA[Cys(COC_8H_{17})NH_2]$_3$ **3** NLC payload*

Prior to NTA[Cys(COC_8H_{17})NH_2]$_3$ **3** NLC payload analysis by HPLC, SPE separation was performed to correctly separate free and NLC-surface weakly bounded compound **3** from firmly NLC-loaded lipophilic pro-chelator **3**, as previously described for cyclosporine A-loaded NLC formulations (Figure S2) (Guillot et al., 2015). Oasis HLB™ SPE cartridges (1 mL, 80 Å pore size, 30 µm particle size) were provided by Waters and connected to a Visiprep™ 12-port vacuum manifold from Supelco. Methanol (4 mL) followed by PBS-1X (6 mL) were first introduced into the SPE-cartridges for cleaning and equilibration prior to the introduction of the formulated samples. The nanoparticles were eluted by PBS 1X (4 mL) in the first fraction (F1). The free drug was eluted by methanol (4 mL) in a second fraction (F2). The nanoparticles eluted in F1 should further be disintegrated to release the entrapped drug. Briefly, the disintegration step consisted in freezing the nanoparticle samples in liquid nitrogen prior to lyophilisation. The resulting solid was solubilized in methanol to reach a

theoretical drug concentration of 1 mg/mL. The drug content was quantified using the suitable HPLC method described above (Figure S3). The free drug eluted in F2 could be directly quantified by HPLC. The total drug content was determined for a sample without being passed through SPE but directly prepared as previously described in the disintegration step (sample F0, Figure S2).

2.6. Cell culture

The HepG2/C3a cell line from ATCC was grown in Minimum Essential Medium (MEM) containing L-glutamine supplemented with 10 % v/v fetal bovine serum (FBS), 100 U/mL penicillin and 100 µg/mL streptomycin. Cells were cultured at 37°C in a humidified atmosphere with 5 % CO_2.

2.7. NLC cellular uptake analysis

The hepatocyte uptake of DiD-loaded NLC was analysed by flow cytometry and confocal fluorescence microscopy as described in (Gauthier et al., 2021).

2.8. MTT viability assay

Cytotoxicity was evaluated using the MTT assay. 1.10^4 cells per well were seeded in a flat-bottom 96-well plate and were incubated for 48 hours at 37°C with 5% CO_2 before addition of copper and chelators or NLC formulation. To determine the LD50 for copper, a concentration series between 0 and 800 µM Cu was used. Copper was added in the form of $CuCl_2$ in the medium in the presence or not of the different chelators, TTM (25 µM); D-pen

(500 µM); trientine (500 µM); **3** (25 or 2 µM); NLC (1.46 or 0.11 mg/mL of lipids); **3**-NLC (1.46 or 0.11 mg/mL of lipids and 25 or 2 µM of pro-chelator **3**). In all experiments, each condition was performed in triplicate in the plate. Besides, each experiment was done three times independently. After 24 hours of incubation in presence of Cu with or without chelators or NLC, medium was discarded, cells were rinsed with PBS and 100 µL of medium containing 0.5 mg/mL of MTT was added to each well. After 1 hour of incubation at 37°C, MTT solution was discarded and formazan crystals formed were dissolved in 150 µL of 4 mM HCl, 0.1 % NP40 in isopropanol. The absorbance in the wells were read in a microplate reader (Tecan microplate reader-550) at 570 nm.

2.9. Quantitative Real Time-Polymerase Chain Reaction

For gene expression studies, $1.5.10^6$ cells were seeded per 6-cm diameter petri dish and were incubated for 24 hours at 37°C with 5% CO_2 before addition of chelators or NLC formulation for 2 hours. Cells were then rinsed with PBS and fresh medium with or without chelator was added. The different chelators were used at the following concentrations: TTM (25 µM); D-pen (200 µM); trientine (200 µM); **3** (25 µM); **3**-NLC (1.46 mg/mL of lipids and 25 µM of pro-chelator). After 2 hours of incubation, medium was removed and cells were rinsed twice with PBS. Fresh medium containing 50 µM copper was added. After 6 hours of incubation with copper, cells were harvested and mRNA were isolated using an Absolutely RNA miniprep kit (Agilent). The RNA concentration was determined using a NanoDrop spectrophotometer (ND-1000). One µg mRNA were reverse transcribed with the Affinity

script qPCR cDNA synthesis kit (Agilent), according to the manufacturer's instructions. The different primers were previously described in (Cuillel et al., 2014). Quantitative PCR was performed with Brilliant II SYBR green qPCR master mix1 (Agilent) and 200 nM primer. PCR reaction mixtures (10 µl) were placed in the Cfx96 instrument (Bio-Rad) where they underwent the following cycling program, optimized for a 96-well block: 95°C for 15 min, immediately followed by 40 cycles of 10 sec at 95°C and 30 sec at 60°C. At the end, PCR products were dissociated by incubating for 1 min at 95°C and then 30 sec at 55°C, followed by a ramp up to 95°C. qRT-PCR reactions were run in triplicate, and quantification was performed using comparative regression (Cq determination mode) using Cfx software (Bio-Rad Cfx manager) with GAPDH and HPRT amplification signals as housekeeping genes to correct for total RNA content and labelling untreated sample as the “calibrator”.

3. Results

3.1. Synthesis of the lipophilic copper pro-chelator NTA(Cys(COC$_8$H$_{17}$)NH$_2$)$_3$ ***3***

To access efficient loading of the copper chelator, NTA(CysNH$_2$)$_3$, in NLC, a lipophilic derivative was prepared by adding C_8H_{17} alkyl chains *via* a thioester link on the thiol functions of NTA(CysNH$_2$)$_3$. This lipophilic derivative NTA(Cys(COC$_8$H$_{17}$)NH$_2$)$_3$ **3** was synthesized according to synthetic Scheme 1. NTA(CysNH$_2$)$_3$ was firstly synthesized according to a previously described procedure in 2 steps with an overall yield of 50% (Pujol et al., 2011b). Then, the C_8H_{17} alkyl chains were introduced *via* a thioester bond using commercial C_8H_{17}COOH and PyBOP as coupling agent to give the desired compound **3** with a yield of 26% (Scheme 1).

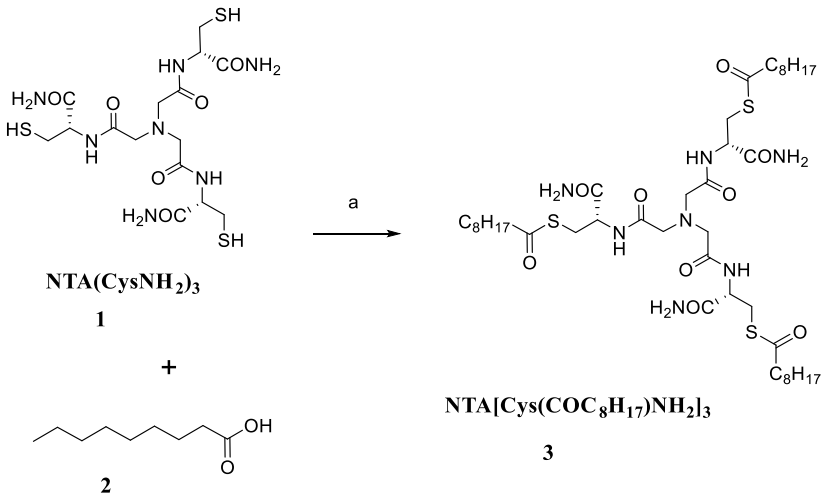

Scheme 1. Synthesis of NTA(Cys(COC_8H_{17})NH_2)$_3$ **3** - Reactants and conditions : a) $C_8H_{17}COOH$, PyBOP, DIEA, DCM, 26%

3.2. Formulation and characterization of nanostructured lipid carriers

NLC were formulated by ultrasonication in the presence or not of 1.8% total weight percentage of NTA(Cys(COC_8H_{17})NH_2)$_3$ **3** according to previously described protocols (Delmas et al., 2011). NLC hydrodynamic diameter and polydispersity index (PDI) were measured by dynamic light scattering (DLS) and are summarized in Table 1. Formulation **3**-NLC, comprising the lipophilic pro-chelator **3**, displayed similar hydrodynamic diameter and PDI than the previously described unloaded NLC particles (Gauthier et al., 2019, 2021). The long-term colloidal stability of formulations was evaluated by the measurement of hydrodynamic diameter and PDI over storage time. **3**-NLC were colloidally stable over at least 6 months (diameter increase < 10%, PDI < 0.2).

Table 1. DLS characterization of NLC and **3**-loaded NLC.

	NLC	**3-NLC**
Hydrodynamic diameter (nm)	42 ± 1	49 ± 1
PDI	0.11 ± 0.02	0.18 ± 0.02
Colloidal stability during storage at 4°C	1 year	> 6 months

NTA(Cys(COC_8H_{17})NH_2)$_3$ **3** NLC payload was quantified by HPLC. Dialysis purification at the end of the fabrication process decreased formulation drug content by approximately 23%, leading to NTA(Cys(COC_8H_{17})NH_2)$_3$ **3** overall encapsulation yield of 72 ± 8% (about 5% of drug was lost during the fabrication process before dialysis). In order to check that the dialysis purification step was efficient and that the lipophilic pro-chelator NTA(Cys(COC_8H_{17})NH_2)$_3$ **3** was indeed incorporated in the core of the NLC and not just weakly bound to the particle surface, solid phase extraction (SPE) was performed to discriminate NLC-core loaded compound **3** from free drug, similarly to previously described protocol (Guillot et al., 2015). Less than 1% of NTA(Cys(COC_8H_{17})NH_2)$_3$ payload was found in the free fraction two weeks after formulation preparation, confirming the efficient and stable loading of the lipophilic pro-chelator in the particle lipid core. In conclusion, NTA(Cys(COC_8H_{17})NH_2)$_3$ **3** drug payload was 1.3% total weight percentage in NLC.

3.3. NLC entry in hepatocytes

The biological activity of NLC was assessed using the hepatoma-derived cell line HepG2/C3a. Fluorescent DiD-loaded NLC were used to confirm the efficient endocytosis of nanoparticles by hepatocytes as shown by flow cytometry (Figure 2a and S4) and confocal fluorescence microscopy (Figure 2b). The former showed that all cells took up NLC within an hour. The latter confirmed that NLC ended up inside the cells and were not bound to the plasma membrane.

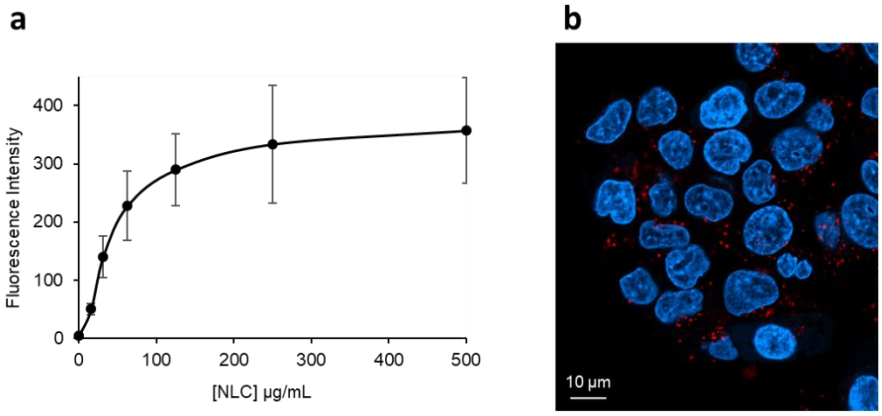

Figure 2. NLC hepatocyte entry. a) Dose-dependent uptake in HepG2/C3a cells of NLC at different concentrations after 30 minutes of exposure. The uptake was measured by flow cytometry and the representation corresponded to the mean fluorescence intensity of the whole cell population as a function of the NLC concentration for each formulation in µg of lipids per mL. **b**) Visualization of NLC cellular uptake in hepatocytes. Confocal fluorescence microscopy of HepG2/C3a cells exposed for 1 hour to 500 µg/mL in lipids of DiD-loaded NLC. Nuclei were labeled with Hoechst (blue) and NLC are visualized in red (DiD).

3.4. *Copper stress protection*

The initial assessment of the toxicity of the different compounds (pro-chelator **3** dispersed in DMSO, **3**-NLC, NLC) showed a gradual and slight decrease of viability up to 25-50 µM of **3** (Figure S5a) and 2.9 mg/mL of lipids (Figure S5b), and a significant toxicity at higher concentration, in particular for **3**. Therefore, a concentration of 25 µM for the pro-chelator **3** was a good compromise for further experiments in presence of copper.

Copper-induced toxicity in HepG2/C3a cells was measured to judge the capacity of compound **3** and **3**-NLC formulation to protect hepatocytes from a copper stress. A standard MTT assay was used to determine the copper concentration required to kill 50% of the cells (LD50) following 24-hour exposure to copper and each compound simultaneously (Figure

3). In standard conditions, without any compound, the LD50 was 457 µM copper, while **3**-NLC (at 25 µM pro-chelator, 1.46 mg/mL of lipids for **3**-NLC) added to the cells enabled a slight protection with a LD50 at 503 µM copper. Interestingly, the free molecule **3** at 25 µM led to a strong and significant protection with a LD50 of 773 µM copper. Empty NLC were also tested to assess their impact on copper toxicity. At a lipid concentration of 1.46 mg/mL, equivalent to **3**-NLC at 25 µM, NLC slightly lowered LD50 to 403 µM copper. This slight increase in toxicity induced by NLC can explain, at least partly, the moderate protection of **3**-NLC. To investigate further the potential of **3**, it was tested at 2 µM and still showed a significant protection with a LD50 of 577 µM copper, while **3**-NLC did not have any effect (LD50 at 437 µM copper). As a comparison, the current molecules used in Wilson's disease therapy, D-pen and trientine added at 500 µM led to LD50 of 653 and 795 µM copper, respectively, which were significant protection against copper stress. High concentrations were used for these two molecules because they are supposed to act outside the cells chelating the labile copper pool as *in vivo*. The Cu(I) chelator under development, TTM, that proved to be effective in copper lowering in liver of Wilson's disease animal models (Czachor et al., 2002) was also tested. It was used at 25 µM as the pro-chelator **3** encapsulated or not and showed only a moderate protection of the cells with a LD50 of 538 µM copper, which was similar to **3**-NLC formulation.

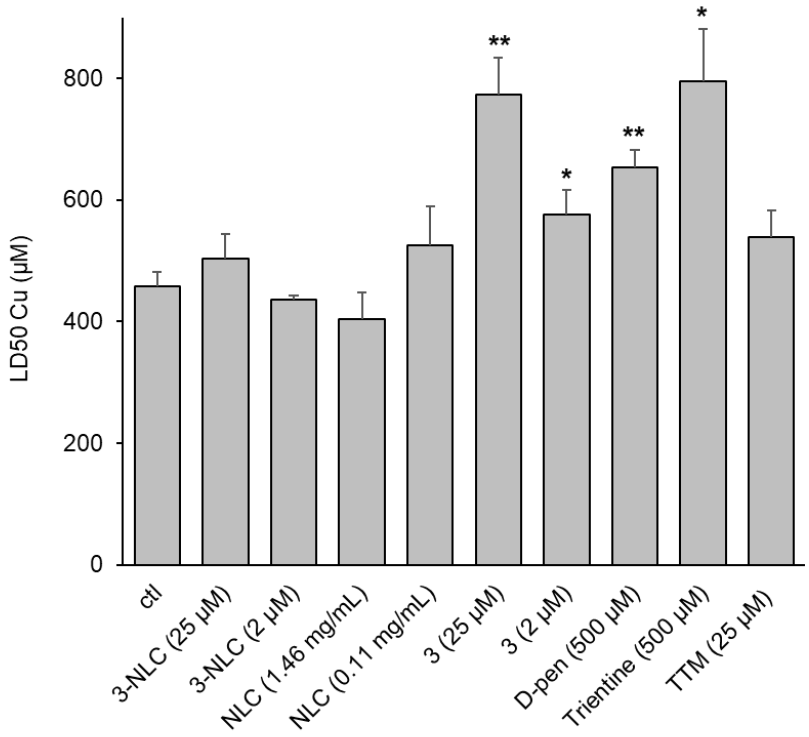

Figure 3. Impact of various chelators and NLC formulations on the lethality induced by copper. The copper dose lethal for 50% of the cells (LD50 copper) was determined by MTT assay on HepG2/C3a cells in presence of the different compounds and NLC at the indicated concentrations. Data presented correspond to the average of at least three independent experiments +/- standard deviation. * stands for data statistically different from the control (ctl) with $p<0.05$ and ** stands for data statistically different from the control with $p<0.01$.

3.5. Cell response to copper and chelators

Quantification of selected mRNA was used to evidence the impact of the different chelators on cell response mechanisms triggered by a moderate copper stress. Cells were incubated during 2 hours with these chelators and without copper. Media was then withdrawn, cells were rinsed to remove the molecules that have not been internalized. Further incubation for 6 hours with 50 µM copper was finally done. The objective was thus to identify the intracellular effect of the different chelators. Metallothioneins (Met) are markers of metal

stress and the expression of the gene coding for Met1X, which is one of the isoform expressed in hepatocytes, is increased 22-fold upon exposure to copper (Figure 4). Interestingly, **3**-NLC and the pro-chelator **3** led to a lower increase of Met1X, 17- and 13-fold, respectively. This suggests that a significant amount of copper was bound to the chelator. Therefore, NLC can release the pro-chelator **3** in hepatic cells and hepatocyte esterases cleave the thioester bond to release the active chelator. As expected for extracellular Cu chelators, D-pen and trientine, they did not protect from the copper stress with Met1X overexpression of 22- and 21-fold, respectively. Finally, TTM significantly increased the metal stress with 31-fold Met1X expression. This effect can be due to the release of Mo in the cell, which is an indirect proof of TTM cellular entry. The expression of the glutamate-cysteine ligase (GCLM) was also assessed (Figure 4). GCLM is the rate-limiting enzyme for the production of glutathione that maintains the intracellular redox potential and plays a role in metal chelation. In this condition, copper had only a very minor impact on GCLM expression with a 1.6-fold increase and the addition of chelator did not have a significant impact except for TTM that increased the expression to 3.5-fold. Since copper can favor oxidative stress inside cells, the expression of heme oxygenase (HMOX), a classical marker of this stress, was also measured (Figure 4). Similarly to GCLM, copper only increased HMOX expression 1.6-fold, and both **3**-NLC and **3** induced an expression above 2, which was a minor effect compared to TTM that triggered a significant oxidative stress with HMOX expression reaching 6.8-fold.

Recently, it was proposed that protein unfolding could be a main impact of copper stress (Saporito-Magriñá et al., 2018). To test this mechanism, the expression of the heat shock

protein HSPA6 was determined (Figure 4). The exposure to copper strongly increased HSPA6 expression, 27-fold, and all the compounds led to similar values except the pro-chelator **3** that significantly decreased HSPA6 expression to reach 14-fold. These results confirm the release of an active chelator from the pro-chelator **3,** this chelator being very efficient to protect cells against a copper stress.

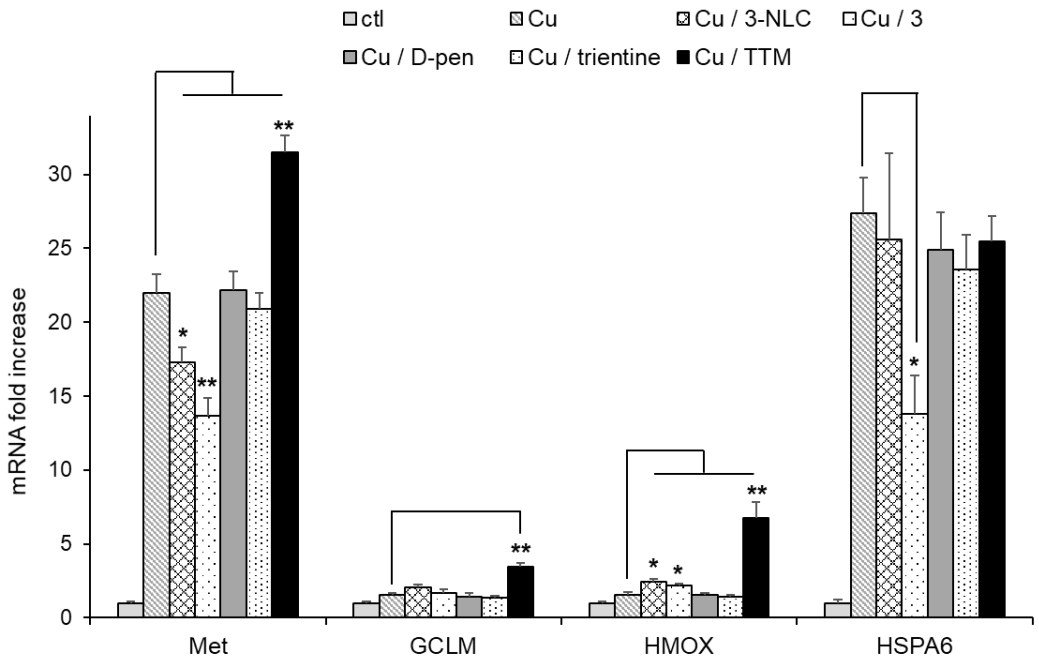

Figure 4. Effect of chelators on the cellular response to copper stress. Met1X, GCLM, HMOX and HSPA6 mRNA fold increase in HepG2/C3a cells exposed first to nothing or the chelators for 2 hours, and second to 50 µM copper for 6 hours after washing the cells out of the chelators. The concentrations used were 25 µM for **3**, **3**-NLC and TTM, and 200 µM for D-pen and trientine. Results are expressed as the relative change in expression compared to the control. The results are expressed as means +/- standard error of the mean of at least three independent experiments. * stands for data statistically different between copper and copper with chelator with $p<0.05$ and ** stands for data statistically different between copper and copper with chelator with $p<0.01$.

4. Discussion

The objective of designing copper-chelators loaded into nanostructured lipid carriers for their efficient transport into hepatocytes for the treatment of Wilson's disease has led us to the synthesis of the original lipophilic copper pro-chelating molecule $NTA(Cys(COC_8H_{17})NH_2)_3$ **3**. This compound was based on $NTA(CysNH_2)_3$, a previously developed Cu(I) chelator inspired from the high affinity Cu(I) binding sites found in metallothioneins that display a CuS_3 trigonal coordination (Pujol et al., 2011b). Three medium length (C8) lipophilic chains were added to the $NTA(CysNH_2)_3$ scaffold via a thioester link to load the pro-chelator into the lipophilic core of NLC, mainly composed of C12 to C18 mono-, di- and triglycerides (Varache et al., 2019). The high and stable encapsulation yield of $NTA(Cys(COC_8H_{17})NH_2)_3$ **3** in NLC (72 ± 8 %) showed the efficient incorporation of the lipophilic pro-chelator into the nanoparticle core.

The biological properties of pro-chelator **3** were assessed in the hepatoma-derived cell line HepG2/C3a, a very good hepatocyte model since it forms active bile canaliculi (Sharma et al., 2020). Since Wilson disease is an evolving pathology with Cu accumulation in liver over years, we decided to compare the biological activity of the different assessed chelators and formulations in two exposure scenarii: i, upon acute Cu level leading to cell death, and ii, upon moderate Cu concentration (50 µM). In the first scenario, hepatocytes were exposed to concentrations higher than those observed in Wilson disease but it enabled to evaluate the ability of the tested molecules and formulation to decorporate liver from Cu in patients with late discovery of the pathology. The second scenario was closer to Cu concentrations encountered in liver of patients suffering from Wilson's disease, and enabled to follow relevant patient biomarkers. Therefore, overall the two tested scenarii were complementary to assess the potential of the different molecules and formulations. Molecule **3** proved to be efficient at low concentration to both protect cells against massive and lethal amounts of

copper, and to decrease metal and protein unfolding stress upon exposure to medium copper concentration, as can be expected during Wilson's disease progression. This efficiency was due to the direct entry of the molecule inside hepatocyte cytosol and the further release of the active chelator trapped inside the cell. This novel molecule was compared to the current clinical standards used against Wilson's disease, *i.e.* D-pen, trientine and TTM. Pro-chelator **3** outclassed those molecules in all assessed criteria. D-pen and trientine were hindered by their extracellular action, proved with mRNA quantification experiments, and that impose to use high doses in treatments that are not well tolerated by all patients. TTM can be used at lower concentrations but showed only a limited protection against a lethal copper stress. Moreover, cellular responses were worsen by TTM that clearly triggered metal and oxidative stress, as evidenced by the increase of the expression of genes coding for Met1X and HMOX, respectively. In comparison, molecule **3** appeared as a promising candidate for Wilson's disease therapy. It could protect from cell death even at 2 µM, and it acted on the main stress induced by copper, in particular against protein unfolding that has now been deciphered as a major impact of intracellular copper excess (Saporito-Magriñá et al., 2018).

To go towards the clinic and take into account the challenge of organismal bioavailability, pro-chelator **3** was formulated into NLC that were efficiently endocytosed by hepatocytes. The biological activity of **3**-NLC was more mitigated than that obtained with non-encapsulated **3** in the same conditions. However, **3**-loaded NLC showed a slight capacity to protect hepatocytes against an acute copper stress at a similar level than TTM. Besides, **3**-NLC significantly decreased metal stress as shown by Met overexpression, which proved that after cellular uptake, the pro-chelator was released from NLC and then processed into an active chelator. It has to be noted that cellular experiments were performed with similar incubation times for compound **3** and **3**-NLC. A longer incubation time could improve NLC

internalization and release of the chelator into cells, and thus the efficiency of these nanovectors that could enable a stronger effect of **3**-NLC against an acute copper stress.

3-NLC formulation could also improve the therapy and treatment compliance thanks to liver accumulation and thereof targeted delivery of the active chelator, which will favour efficiency and prolonged action. In this perspective, we explored the loading of compound **3** in a first formulation of nanostructured lipid carriers. This first formulation could be further optimized to take full benefit of the promising cellular properties of compound **3**. For instance, the choice of the lipids entering the NLC composition could be adjusted to improve the pro-chelator encapsulation yield, allowing to improve as well drug payload and reduce the quantity of lipid excipients. With this first set of cellular results in hand, *in vivo* experiments are also seeked to explore the full benefit of the NLC-based strategy for parenteral or oral administration of pro-chelator **3**. The nanovector-based strategy is expected to avoid current side effects observed with conventional presently-used chelators, that distribute everywhere in the organism, and are therefore administered at high concentrations to reach effective dose in the liver targeted organ. Future experiments will therefore be conducted in the direction of the nanovectorization of compound **3**, with the ultimate goal to offer new therapeutic options for patients suffering from Wilson's disease.

5. Conclusion

In summary, we herein showed that $NTA(Cys(COC_8H_{17})NH_2)_3$ compound **3** appears a very promising molecule to study in the context of Wilson's disease. Indeed, in the cellular assays presented here, the molecule was superior to the current and in development therapies to cope with copper stress in a safe way as opposed to TTM. Additionally, its lipophilic structure could advantageously be used to quantitatively load the drug into lipid nanocarriers to convey

it more efficiently to its site of action, namely hepatocytes, after parenteral or oral administration.

Acknowledgments

We thank Veronique Collin-Faure for her support for flow cytometry experiments. This project received funding from GRAL and Arcane Labex, programs from the Chemistry Biology Health (CBH) Graduate School of University Grenoble Alpes (ANR-17-EURE-0003) and Glyco@Alps "Investissement d'avenir" program (ANR-15-IDEX-02). This work was also supported by the Région Auvergne Rhône-Alpes (PhD grant for L.G.).

Author contribution

LG performed chemical synthesis, NLC encapsulation and FACS experiments. PC, MC and AD performed cellular experiments. LG, MC, PD, IT, CG and AD analyzed the data. PD, IT, CG and AD designed the study and wrote the manuscript.

Declaration of interest

The authors declare that they have no known competing financial interests or personal relationships that could have appeared to influence the work reported in this paper.

References

Allocca, S., Ciano, M., Ciardulli, M., D'Ambrosio, C., Scaloni, A., Sarnataro, D., Caporaso, M., D'Agostino, M., Bonatti, S., 2018. An αB-Crystallin Peptide Rescues Compartmentalization and Trafficking Response to Cu Overload of ATP7B-

H1069Q, the Most Frequent Cause of Wilson Disease in the Caucasian Population. Int. J. Mol. Sci. 19, 1892. https://doi.org/10.3390/ijms19071892

Bayon, E., Morlieras, J., Dereuddre-Bosquet, N., Gonon, A., Gosse, L., Courant, T., Le Grand, R., Marche, P.N., Navarro, F.P., 2018. Overcoming immunogenicity issues of HIV p24 antigen by the use of innovative nanostructured lipid carriers as delivery systems: evidences in mice and non-human primates. Npj Vaccines 3. https://doi.org/10.1038/s41541-018-0086-0

Beloqui, A., Solinís, M.Á., Rodríguez-Gascón, A., Almeida, A.J., Préat, V., 2016. Nanostructured lipid carriers: Promising drug delivery systems for future clinics. Nanomedicine Nanotechnol. Biol. Med. 12, 143–161. https://doi.org/10.1016/j.nano.2015.09.004

Carbone, C., Leonardi, A., Cupri, S., Puglisi, G., Pignatello, R., 2014. Pharmaceutical and biomedical applications of lipid-based nanocarriers. Pharm. Pat. Anal. 3, 199–215. https://doi.org/10.4155/ppa.13.79

Cavalli, R., Marengo, E., Rodriguez, L., Gasco, M., 1996. Effects of some experimental factors on the production process of solid lipid nanoparticles. Eur J Pharm Biopharm 110–115.

Cuillel, M., Chevallet, M., Charbonnier, P., Fauquant, C., Pignot-Paintrand, I., Arnaud, J., Cassio, D., Michaud-Soret, I., Mintz, E., 2014. Interference of CuO nanoparticles with metal homeostasis in hepatocytes under sub-toxic conditions. Nanoscale 6, 1707–1715. https://doi.org/10.1039/C3NR05041F

Czachor, J.D., Cherian, M.G., Koropatnick, J., 2002. Reduction of copper and metallothionein in toxic milk mice by tetrathiomolybdate, but not deferiprone. J. Inorg. Biochem. 88, 213–222. https://doi.org/10.1016/S0162-0134(01)00383-X

Członkowska, A., Litwin, T., Dusek, P., Ferenci, P., Lutsenko, S., Medici, V., Rybakowski, J.K., Weiss, K.H., Schilsky, M.L., 2018. Wilson disease. Nat. Rev. Dis. Primer 4, 21. https://doi.org/10.1038/s41572-018-0018-3

Delangle, P., Mintz, E., 2012. Chelation therapy in Wilson's disease: from d-penicillamine to the design of selective bioinspired intracellular Cu(i) chelators. Dalton Trans. 41, 6359. https://doi.org/10.1039/c2dt12188c

Delmas, T., Couffin, A.-C., Bayle, P.A., Crécy, F. de, Neumann, E., Vinet, F., Bardet, M., Bibette, J., Texier, I., 2011. Preparation and characterization of highly stable lipid nanoparticles with amorphous core of tuneable viscosity. J. Colloid Interface Sci. 360, 471–481. https://doi.org/10.1016/j.jcis.2011.04.080

Doktorovová, S., Kovačević, A.B., Garcia, M.L., Souto, E.B., 2016. Preclinical safety of solid lipid nanoparticles and nanostructured lipid carriers: Current evidence from in vitro and in vivo evaluation. Eur. J. Pharm. Biopharm. 108, 235–252. https://doi.org/10.1016/j.ejpb.2016.08.001

Gateau, C., Delangle, P., 2014. Design of intrahepatocyte copper(I) chelators as drug candidates for Wilson's disease: Intracellular copper chelation. Ann. N. Y. Acad. Sci. 1315, 30–36. https://doi.org/10.1111/nyas.12379

Gauthier, L., Chevallet, M., Bulteau, F., Thépaut, M., Delangle, P., Fieschi, F., Vivès, C., Texier, I., Deniaud, A., Gateau, C., 2021. Lectin recognition and hepatocyte

endocytosis of GalNAc-decorated nanostructured lipid carriers. J. Drug Target. 29, 99–107. https://doi.org/10.1080/1061186X.2020.1806286

Gauthier, Varache, Couffin, Lebrun, Delangle, Gateau, Texier, 2019. Quantification of Surface GalNAc Ligands Decorating Nanostructured Lipid Carriers by UPLC-ELSD. Int. J. Mol. Sci. 20, 5669. https://doi.org/10.3390/ijms20225669

Guillot, A., Couffin, A.-C., Sejean, X., Navarro, F., Limberger, M., Lehr, C.-M., 2015. Solid Phase Extraction as an Innovative Separation Method for Measuring Free and Entrapped Drug in Lipid Nanoparticles. Pharm. Res. 32, 3999–4009. https://doi.org/10.1007/s11095-015-1761-8

H. Muller, R., Shegokar, R., M. Keck, C., 2011. 20 Years of Lipid Nanoparticles (SLN & NLC): Present State of Development & Industrial Applications. Curr. Drug Discov. Technol. 8, 207–227. https://doi.org/10.2174/157016311796799062

Ji, H.-F., Shen, L., 2010. Potential of curcumin as a multifunctional agent to combat Wilson disease. Hepatology 51, 2226–2226. https://doi.org/10.1002/hep.23675

Jullien, A.-S., Gateau, C., Kieffer, I., Testemale, D., Delangle, P., 2013. X-ray Absorption Spectroscopy Proves the Trigonal-Planar Sulfur-Only Coordination of Copper(I) with High-Affinity Tripodal Pseudopeptides. Inorg. Chem. 52, 9954–9961. https://doi.org/10.1021/ic401206u

Jullien, A.-S., Gateau, C., Lebrun, C., Delangle, P., 2015. Pseudo-peptides Based on Methyl Cysteine or Methionine Inspired from Mets Motifs Found in the Copper Transporter Ctr1. Inorg. Chem. 54, 2339–2344. https://doi.org/10.1021/ic502962d

Jullien, A.-S., Gateau, C., Lebrun, C., Kieffer, I., Testemale, D., Delangle, P., 2014. D -Penicillamine Tripodal Derivatives as Efficient Copper(I) Chelators. Inorg. Chem. 53, 5229–5239. https://doi.org/10.1021/ic5004319

Kong, W.H., Park, K., Lee, M.-Y., Lee, H., Sung, D.K., Hahn, S.K., 2013. Cationic solid lipid nanoparticles derived from apolipoprotein-free LDLs for target specific systemic treatment of liver fibrosis. Biomaterials 34, 542–551. https://doi.org/10.1016/j.biomaterials.2012.09.067

Krishnan, N., Felice, C., Rivera, K., Pappin, D.J., Tonks, N.K., 2018. DPM-1001 decreased copper levels and ameliorated deficits in a mouse model of Wilson's disease. Genes Dev. 32, 944–952. https://doi.org/10.1101/gad.314658.118

Lichtmannegger, J., Leitzinger, C., Wimmer, R., Schmitt, S., Schulz, S., Kabiri, Y., Eberhagen, C., Rieder, T., Janik, D., Neff, F., Straub, B.K., Schirmacher, P., DiSpirito, A.A., Bandow, N., Baral, B.S., Flatley, A., Kremmer, E., Denk, G., Reiter, F.P., Hohenester, S., Eckardt-Schupp, F., Dencher, N.A., Adamski, J., Sauer, V., Niemietz, C., Schmidt, H.H.J., Merle, U., Gotthardt, D.N., Kroemer, G., Weiss, K.H., Zischka, H., 2016. Methanobactin reverses acute liver failure in a rat model of Wilson disease. J. Clin. Invest. 126, 2721–2735. https://doi.org/10.1172/JCI85226

Liu, L., Tang, Y., Gao, C., Li, Y., Chen, S., Xiong, T., Li, J., Du, M., Gong, Z., Chen, H., Liu, L., Yao, P., 2014. Characterization and biodistribution in vivo of quercetin-loaded cationic nanostructured lipid carriers. Colloids Surf. B Biointerfaces 115, 125–131. https://doi.org/10.1016/j.colsurfb.2013.11.029

Lutsenko, S., 2014. Modifying factors and phenotypic diversity in Wilson's disease: Modifying factors in Wilson's disease. Ann. N. Y. Acad. Sci. 1315, 56–63. https://doi.org/10.1111/nyas.12420

Mehnert, W., 2001. Solid lipid nanoparticles Production, characterization and applications. Adv. Drug Deliv. Rev. 47, 165–196. https://doi.org/10.1016/S0169-409X(01)00105-3

Merian, J., Boisgard, R., Decleves, X., Theze, B., Texier, I., Tavitian, B., 2013. Synthetic Lipid Nanoparticles Targeting Steroid Organs. J. Nucl. Med. 54, 1996–2003. https://doi.org/10.2967/jnumed.113.121657

Michy, Massias, Bernard, Vanwonterghem, Henry, Guidetti, Royal, Coll, Texier, Josserand, Hurbin, 2019. Verteporfin-Loaded Lipid Nanoparticles Improve Ovarian Cancer Photodynamic Therapy In Vitro and In Vivo. Cancers 11, 1760. https://doi.org/10.3390/cancers11111760

Monestier, M., Charbonnier, P., Gateau, C., Cuillel, M., Robert, F., Lebrun, C., Mintz, E., Renaudet, O., Delangle, P., 2016. ASGPR-Mediated Uptake of Multivalent Glycoconjugates for Drug Delivery in Hepatocytes. Chembiochem Eur. J. Chem. Biol. 17, 590–594. https://doi.org/10.1002/cbic.201600023

Monestier, M., Pujol, A.M., Lamboux, A., Cuillel, M., Pignot-Paintrand, I., Cassio, D., Charbonnier, P., Um, K., Harel, A., Bohic, S., Gateau, C., Balter, V., Brun, V., Delangle, P., Mintz, E., 2020. A liver-targeting Cu(I) chelator relocates Cu in hepatocytes and promotes Cu excretion in a murine model of Wilson's disease. Metallomics 12, 1000–1008. https://doi.org/10.1039/D0MT00069H

Müller, R.., Radtke, M., Wissing, S.., 2002. Nanostructured lipid matrices for improved microencapsulation of drugs. Int. J. Pharm. 242, 121–128. https://doi.org/10.1016/S0378-5173(02)00180-1

Murillo, O., Luqui, D.M., Gazquez, C., Martinez-Espartosa, D., Navarro-Blasco, I., Monreal, J.I., Guembe, L., Moreno-Cermeño, A., Corrales, F.J., Prieto, J., Hernandez-Alcoceba, R., Gonzalez-Aseguinolaza, G., 2016. Long-term metabolic correction of Wilson's disease in a murine model by gene therapy. J. Hepatol. 64, 419–426. https://doi.org/10.1016/j.jhep.2015.09.014

Murillo, O., Moreno, D., Gazquez, C., Barberia, M., Cenzano, I., Navarro, I., Uriarte, I., Sebastian, V., Arruebo, M., Ferrer, V., Bénichou, B., Combal, J.P., Prieto, J., Hernandez-Alcoceba, R., Gonzalez Aseguinolaza, G., 2019. Liver Expression of a MiniATP7B Gene Results in Long-Term Restoration of Copper Homeostasis in a Wilson Disease Model in Mice. Hepatology. https://doi.org/10.1002/hep.30535

Nasirizadeh, S., Malaekeh-Nikouei, B., 2020. Solid lipid nanoparticles and nanostructured lipid carriers in oral cancer drug delivery. J. Drug Deliv. Sci. Technol. 55, 101458. https://doi.org/10.1016/j.jddst.2019.101458

Polishchuk, E.V., Concilli, M., Iacobacci, S., Chesi, G., Pastore, N., Piccolo, P., Paladino, S., Baldantoni, D., van IJzendoorn, S.C.D., Chan, J., Chang, C.J., Amoresano, A., Pane, F., Pucci, P., Tarallo, A., Parenti, G., Brunetti-Pierri, N., Settembre, C., Ballabio, A., Polishchuk, R.S., 2014. Wilson disease protein ATP7B utilizes lysosomal exocytosis

to maintain copper homeostasis. Dev. Cell 29, 686–700. https://doi.org/10.1016/j.devcel.2014.04.033

Pujol, A.M., Cuillel, M., Jullien, A.-S., Lebrun, C., Cassio, D., Mintz, E., Gateau, C., Delangle, P., 2012. A sulfur tripod glycoconjugate that releases a high-affinity copper chelator in hepatocytes. Angew. Chem. Int. Ed Engl. 51, 7445–7448. https://doi.org/10.1002/anie.201203255

Pujol, A.M., Cuillel, M., Renaudet, O., Lebrun, C., Charbonnier, P., Cassio, D., Gateau, C., Dumy, P., Mintz, E., Delangle, P., 2011a. Hepatocyte targeting and intracellular copper chelation by a thiol-containing glycocyclopeptide. J. Am. Chem. Soc. 133, 286–296. https://doi.org/10.1021/ja106206z

Pujol, A.M., Gateau, C., Lebrun, C., Delangle, P., 2011b. A Series of Tripodal Cysteine Derivatives as Water-Soluble Chelators that are Highly Selective for Copper(I). Chem. – Eur. J. 17, 4418–4428. https://doi.org/10.1002/chem.201003613

Pujol, A.M., Gateau, C., Lebrun, C., Delangle, P., 2009. A Cysteine-Based Tripodal Chelator with a High Affinity and Selectivity for Copper(I). J. Am. Chem. Soc. 131, 6928–6929. https://doi.org/10.1021/ja901700a

Rae, T.D., Schmidt, P.J., Pufahl, R.A., Culotta, V.C., O'Halloran, T.V., 1999. Undetectable intracellular free copper: the requirement of a copper chaperone for superoxide dismutase. Science 284, 805–808. https://doi.org/10.1126/science.284.5415.805

Saporito-Magriñá, C.M., Musacco-Sebio, R.N., Andrieux, G., Kook, L., Orrego, M.T., Tuttolomondo, M.V., Desimone, M.F., Boerries, M., Borner, C., Repetto, M.G., 2018. Copper-induced cell death and the protective role of glutathione: the implication of impaired protein folding rather than oxidative stress. Metallomics 10, 1743–1754. https://doi.org/10.1039/C8MT00182K

Sawant, K., Dodiya, S., 2008. Recent Advances and Patents on Solid Lipid Nanoparticles. Recent Pat. Drug Deliv. Formul. 2, 120–135. https://doi.org/10.2174/187221108784534081

Sayag, D., Cabon, Q., Texier, I., Navarro, F.P., Boisgard, R., Virieux-Watrelot, D., Carozzo, C., Ponce, F., 2016. Phase-0/phase-I study of dye-loaded lipid nanoparticles for near-infrared fluorescence imaging in healthy dogs. Eur. J. Pharm. Biopharm. 100, 85–93. https://doi.org/10.1016/j.ejpb.2016.01.001

Sharma, V.R., Shrivastava, A., Gallet, B., Karepina, E., Charbonnier, P., Chevallet, M., Jouneau, P.-H., Deniaud, A., 2020. Canalicular domain structure and function in matrix-free hepatic spheroids. Biomater. Sci. 8, 485–496. https://doi.org/10.1039/C9BM01143A

Tan, J.S.L., Roberts, C., Billa, N., 2020. Pharmacokinetics and tissue distribution of an orally administered mucoadhesive chitosan-coated amphotericin B-Loaded nanostructured lipid carrier (NLC) in rats. J. Biomater. Sci. Polym. Ed. 31, 141–154. https://doi.org/10.1080/09205063.2019.1680926

Teixeira, M.C., Carbone, C., Souto, E.B., 2017. Beyond liposomes: Recent advances on lipid based nanostructures for poorly soluble/poorly permeable drug delivery. Prog. Lipid Res. 68, 1–11. https://doi.org/10.1016/j.plipres.2017.07.001

Tezgel, Ö., Szarpak-Jankowska, A., Arnould, A., Auzély-Velty, R., Texier, I., 2018. Chitosan-lipid nanoparticles (CS-LNPs): Application to siRNA delivery. J. Colloid Interface Sci. 510, 45–56. https://doi.org/10.1016/j.jcis.2017.09.045

Tremmel, R., Uhl, P., Helm, F., Wupperfeld, D., Sauter, M., Mier, W., Stremmel, W., Hofhaus, G., Fricker, G., 2016. Delivery of Copper-chelating Trientine (TETA) to the central nervous system by surface modified liposomes. Int. J. Pharm. 512, 87–95. https://doi.org/10.1016/j.ijpharm.2016.08.040

van den Berghe, P.V.E., Stapelbroek, J.M., Krieger, E., de Bie, P., van de Graaf, S.F.J., de Groot, R.E.A., van Beurden, E., Spijker, E., Houwen, R.H.J., Berger, R., Klomp, L.W.J., 2009. Reduced expression of ATP7B affected by Wilson disease-causing mutations is rescued by pharmacological folding chaperones 4-phenylbutyrate and curcumin. Hepatology 50, 1783–1795. https://doi.org/10.1002/hep.23209

Varache, M., Ciancone, M., Couffin, A.-C., 2019. Development and validation of a novel UPLC-ELSD method for the assessment of lipid composition of nanomedicine formulation. Int. J. Pharm. 566, 11–23. https://doi.org/10.1016/j.ijpharm.2019.05.038

Vigne, J., Cabella, C., Dézsi, L., Rustique, E., Couffin, A.-C., Aid, R., Anizan, N., Chauvierre, C., Letourneur, D., Le Guludec, D., Rouzet, F., Hyafil, F., Mészáros, T., Fülöp, T., Szebeni, J., Cordaro, A., Oliva, P., Mourier, V., Texier, I., 2020. Nanostructured lipid carriers accumulate in atherosclerotic plaques of ApoE−/− mice. Nanomedicine Nanotechnol. Biol. Med. 25, 102157. https://doi.org/10.1016/j.nano.2020.102157

Wang, F., He, Z., Dai, W., Li, Q., Liu, X., Zhang, Z., Zhai, D., Chen, J., Chen, W., 2015. The role of the vascular endothelial growth factor/vascular endothelial growth factor receptors axis mediated angiogenesis in curcumin-loaded nanostructured lipid carriers induced human HepG2 cells apoptosis. J. Cancer Res. Ther. 11, 597. https://doi.org/10.4103/0973-1482.159086

Weiss, K.H., Askari, F.K., Czlonkowska, A., Ferenci, P., Bronstein, J.M., Bega, D., Ala, A., Nicholl, D., Flint, S., Olsson, L., Plitz, T., Bjartmar, C., Schilsky, M.L., 2017. Bis-choline tetrathiomolybdate in patients with Wilson's disease: an open-label, multicentre, phase 2 study. Lancet Gastroenterol. Hepatol. 2, 869–876. https://doi.org/10.1016/S2468-1253(17)30293-5

Wilson, S.A.K., 1912. PROGRESSIVE LENTICULAR DEGENERATION: A FAMILIAL NERVOUS DISEASE ASSOCIATED WITH CIRRHOSIS OF THE LIVER. Brain 34, 295–507. https://doi.org/10.1093/brain/34.4.295